

Dielectric Comline Resonators and Filters

Chi Wang, *Senior Member, IEEE*, Kawthar A. Zaki, *Fellow, IEEE*,
Ali E. Atia, *Fellow, IEEE*, and Tim G. Dolan

Abstract—The dielectric comline resonator combines the merits of the metallic comline and dielectric loaded resonator. By replacing the inner conductor of the conventional comline resonator by a high ϵ_r dielectric rod, higher unloaded Q can be expected. Resonant frequency, unloaded Q , and coupling coefficient of the resonator are obtained by a rigorous mode-matching method. An eight-pole elliptic-function dielectric comline resonator filter was designed and tested. Measured frequency responses verify the theory.

Index Terms—Comline resonator, dielectric resonator filter, filter, wireless communications filter.

I. INTRODUCTION

HIGH-PERFORMANCE microwave cavity filters are finding increasing applications in satellite and mobile communication systems. Coaxial comline resonator filters and dielectric loaded resonator filters are commonly used in the systems because of small size and their unique characteristics. Coaxial resonators have low cost, wide tuning range, and excellent spurious-free performance [1], [2], [11], while dielectric loaded resonator filters have very low loss and high-temperature stability [3]–[6]. However, the drawback of the comline resonator filters is their relatively high loss, due to the low unloaded Q of the resonator, while the dielectric loaded resonator has higher cost and poor spurious performance.

The low unloaded Q of the comline resonator is mostly due to the additional conducting loss dissipated on the inner conductor compared with the dielectric loaded resonator due to the quasi-TEM characteristics of the resonator. The electromagnetic fields varies according to $1/r$ relation along the radial direction. As a result, large current is induced on the surface of the inner conductor, and it limits the unloaded Q of the coaxial resonator. The metallized quarter-wavelength dielectric resonators give much lower unloaded Q because of the strong field and the high conductive loss even with very low-loss dielectric material [7], [8].

However, the perfect conducting boundary condition (PEC) can be replaced by dielectric material with infinite dielectric constant ($\epsilon_r \rightarrow \infty$) [12]. Although infinite dielectric-constant material cannot be obtained, dielectrics with high relative dielectric constant can achieve similar condition. Since the

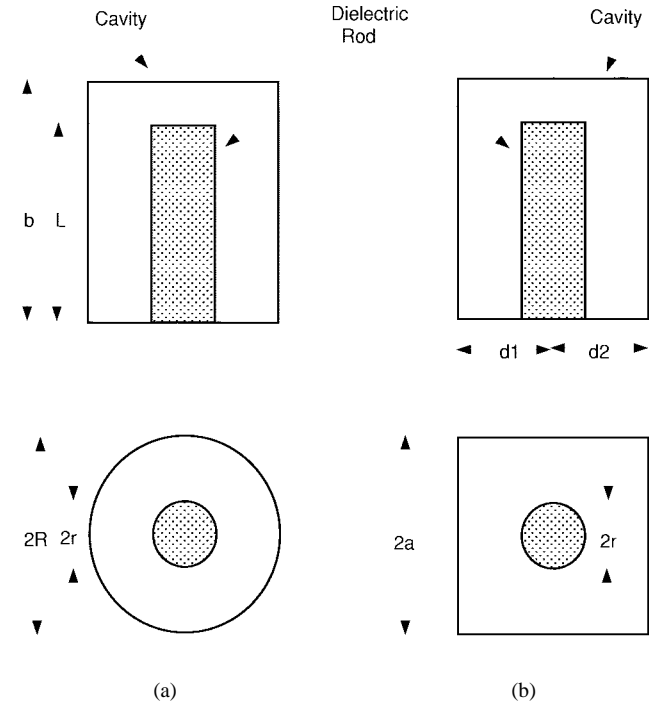


Fig. 1. Configurations of the dielectric comline resonators. (a) Cylindrical enclosure. (b) Rectangular enclosure.

magnetic field is continuous at the boundary of the dielectrics, no electric current is induced on the dielectric rod, thus, higher unloaded Q can be expected.

In this paper, a novel type of coaxial resonator, i.e., the dielectric comline resonator, is introduced by replacing the inner conductor of the conventional comline resonator by a high ϵ_r dielectric rod. The new type of resonator has higher unloaded Q and the merits of the metallic comline resonator and dielectric loaded resonator. A rigorous mode-matching method is used to compute the resonant frequency, unloaded Q , and coupling coefficient of the resonators. The dielectric comline resonator can be used to fully or partially replace the metallic comline resonators in the filters. Properties of this new type of resonator are extensively investigated. An eight-pole elliptic-function dielectric-comline-resonator filter was designed, and verified the theory.

Manuscript received March 27, 1998; revised August 28, 1998.

C. Wang is with the Celwave, Division, Radio Frequency System Inc., Marlboro, NJ 07746 USA.

K. A. Zaki is with the Department of Electrical Engineering, University of Maryland at College Park, College Park, MD 20742 USA.

A. E. Atia is with Orbital Sciences Incorporated, Germantown, MD 20874 USA.

T. G. Dolan is with K & L Microwave Inc., Salisbury, MD 21801 USA.
Publisher Item Identifier S 0018-9480(98)09237-0.

II. CONFIGURATION AND ANALYSIS

The typical configurations of the dielectric comline resonators are shown in Fig. 1. A dielectric rod with radius r and length L is mounted in a cylindrical or rectangular enclosure of length b . The inner dielectric rod can also be rectangular or

other cross section in shape depending on the manufacturing process.

A rigorous mode-matching method is used for modeling of the dielectric combline resonators, shown in Fig. 1(a) and (b). The difference between the two kinds of resonators is that the resonator of Fig. 1(a) has a cylindrical sidewall, while the enclosure of the resonator in Fig. 1(b) is rectangular. By placing an artificial cylindrical boundary [10], [11] at $\rho = a$ of the rectangular enclosure resonator, the structure is divided into the cylindrical and waveguide regions. In both structures, the cylindrical regions are the same, which can be further divided into two subregions: two-layer region I ($\rho \leq r$) and one-layer region II ($r < \rho \leq R$ or a).

The fields in each cylindrical region can be expanded by TE_y and TM_y modes of parallel planes bounded in the y -direction in a cylindrical coordinate system (ρ, ϕ, y) [6], while the fields in the rectangular regions are expanded into the summations of the TE_z and TM_z modes in the rectangular waveguide in the Cartesian coordinate system (x, y, z) . The normal fields in each region satisfy the wave equations in the charge-free region in their own coordinate system as

$$\nabla^2 E_n^e + k^2 E_n^e = 0 \quad (1)$$

$$\nabla^2 H_n^h + k^2 H_n^h = 0 \quad (2)$$

$$k = \omega \sqrt{\mu \epsilon} \quad (3)$$

where E_n^e represents the normal-field component of TM mode, and H_n^h represents the normal-field component of TM mode, respectively. Solving the wave equations, the normal fields can be obtained, and the other field components can be derived from the normal electric or magnetic field.

The tangential electromagnetic fields in the waveguide regions at the artificial boundary $\rho = a$ can be expressed as

$$\vec{E}_{wt}^{iq}(\rho, \phi, y) = -\hat{\rho} \times (\hat{\rho} \times \vec{E}_w^{iq}(x, y, z)|_{x^2+z^2=a^2}) \quad (4)$$

$$\vec{H}_{wt}^{iq}(\rho, \phi, y) = -\hat{\rho} \times (\hat{\rho} \times \vec{H}_w^{iq}(x, y, z)|_{x^2+z^2=a^2})$$

$$i = w_1 \text{ or } w_2$$

$$q = e \text{ or } h \quad (5)$$

in order to be able to match the electromagnetic fields between the cylindrical and rectangular regions.

Forcing the tangential E - and H -fields to be continuous at the interface between the cylindrical regions and taking the proper inner products, one can obtain the field coefficient equation of the cylindrical region as

$$[M_C^{\text{II}}][C^{\text{II}}] + [M_D^{\text{II}}][D^{\text{II}}] = 0 \quad (6)$$

where $[C^{\text{II}}]$ and $[D^{\text{II}}]$ are field coefficient vectors related to the inner going and the outgoing cylindrical waves in region II.

For a cylindrical enclosure structure, $[M_C^{\text{II}}]$ and $[M_D^{\text{II}}]$ are block matrices corresponding to the inner products of the eigenmodes of the specified ϕ variation. By applying a boundary condition at R , a characteristic equation can be obtained as

$$\det [X]_{N_{\text{II}} \times N_{\text{II}}} = 0. \quad (7)$$

TABLE I
UNLOADED Q OF A CONVENTIONAL COMBLINE RESONATOR ($r = 0.21$ in, $L = 1.1$ in) AND A DIELECTRIC COMBLINE RESONATOR ($r = 0.28$ in, $L = 1.20$ in), DUE TO THE INNER ROD AND ENCLOSURE WITH $f_o = 1.87$ GHz,
 $R = 0.75$ in, $b = 1.26$ in, $\sigma = 15.67 \times 10^5$ U/in AND $\tan \delta = 4.0 \times 10^{-5}$

Region	Combline	DR combline
Rod Q	9733.2	39064.6
Enclosure Q	13146.0	13578.6
Total Q	5592.5	10076.2

Solving the equation gives the resonant frequency and field expansion coefficients of each region. The unloaded Q of the cavity can then be computed analytically by integrating the superposition of the eigenmode fields. The coupling coefficient between two cylindrical cavities is obtained by using the improved large-aperture coupling theory considering the iris width factor [13]–[15].

For rectangular enclosure structure, $[M_C^{\text{II}}]$ and $[M_D^{\text{II}}]$ are diagonal block matrices. Each block matrix corresponds to the inner products of the eigenmodes with a ϕ variation. The fields outside the boundary are linear combinations of the waveguide eigenmodes, including both incident and reflected waves. The waveguide eigenmodes are expanded by Bessel–Fourier series so that they can be expressed in the cylindrical coordinate system and all the integrals involved in the mode-matching procedure can be evaluated analytically.

Applying boundary conditions at the artificial boundary, taking the proper inner products, and after some matrix operation, a matrix equation relating the field coefficients of the incident and reflected waves in the waveguide regions w_1 and w_2 to the coefficients of cylindrical region II can be obtained, following [11], as

$$\begin{bmatrix} C^{\text{II}} \\ D^{\text{II}} \end{bmatrix} = \begin{bmatrix} [M_A^{11}] & [M_A^{12}] \\ [M_A^{11}] & [M_A^{12}] \end{bmatrix} \begin{bmatrix} A^{w_1} \\ A^{w_2} \end{bmatrix} + \begin{bmatrix} [M_B^{11}] & [M_B^{12}] \\ [M_B^{11}] & [M_B^{12}] \end{bmatrix} \begin{bmatrix} B^{w_1} \\ B^{w_2} \end{bmatrix} \quad (8)$$

where A and B are the field coefficients of the incident and reflected waves in the waveguide regions w_1 and w_2 .

From (6) and (8), the desired generalized scattering matrix of the conductor loaded resonator in a rectangular waveguide can be obtained. Once the S -matrices of the structure are known, the cascading procedure of S -matrices may be employed to obtain the eigen equations for the resonant frequencies of a single cavity and of two identical slot-coupled cavities. The coupling coefficient can then be computed from the two resonant frequencies f_e and f_m with PEC and perfect magnetic conductor (PMC) placed at the $x = 0$ plane, respectively, as

$$k = \frac{M}{L} = \frac{f_e^2 - f_m^2}{f_e^2 + f_m^2}. \quad (9)$$

III. NUMERICAL RESULTS

Table I shows the typical computed unloaded Q of a conventional combline resonator and a dielectric combline resonator with the same enclosure dimensions and resonant frequency. It is seen that both the inner and outer conductor

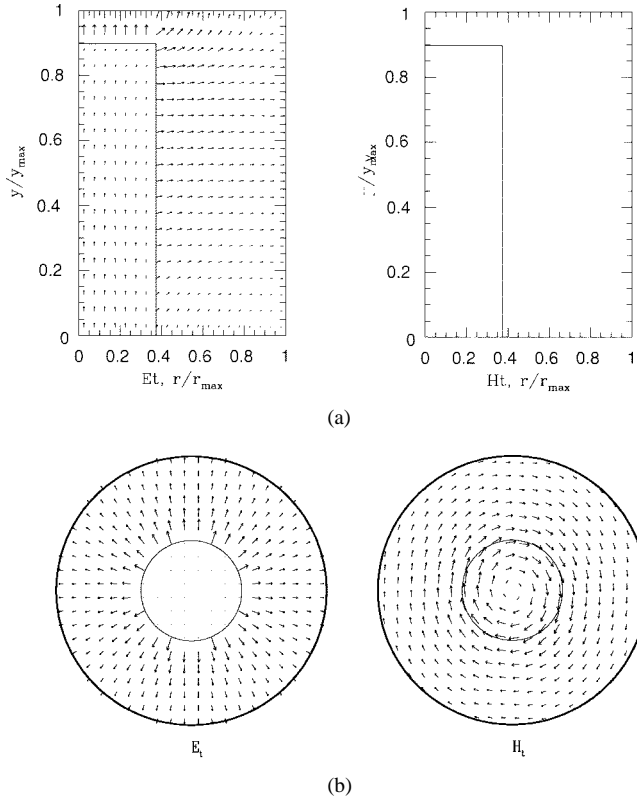


Fig. 2. Field distributions of a dielectric combline resonator. (a) $r - y$ plane. (b) $r - \phi$ plane.

of a conventional combline resonator contribute approximately the same loss to the resonator, which results in the relatively low unloaded Q of the combline resonator. The loss due to the dielectric rod of the dielectric combline resonator is very small, thus the dielectric combline resonator has nearly twice the unloaded Q as that of the conventional combline resonator.

Fig. 2 shows the typical field distributions of a dielectric combline resonator with cylindrical enclosure in the $r - y$ and the $r - \phi$ planes. It is seen that, as expected, both electric and magnetic fields in the air-filled region are quite similar to that of the metallic resonator. Within the dielectric rod, electric field E_y and magnetic field H_ϕ exist. The continuous magnetic field at the boundary eliminates the current on the dielectric rod.

The computed resonant frequency and the unloaded Q of a dielectric combline resonator versus the radius of the dielectric rod and with different length of the rod are presented in Figs. 3 and 4, respectively. Both resonant frequency and the unloaded Q decrease as the radius and length of the dielectric rod increases. Unlike metallic combline resonators, there is no optimum value of the inner and outer radius ratio, which gives the maximum unloaded Q . The resonators have much higher unloaded Q than that of the conventional combline resonators.

The mode charts have been computed to analyze the resonator. Fig. 5 presents the dependence of the resonant modes on the radius of the dielectric rod. It is seen that all the resonant modes are sensitive to the rod diameter. Dielectric rod with smaller radius has better mode separation. Fig. 6 shows the mode chart of the resonator with the length of

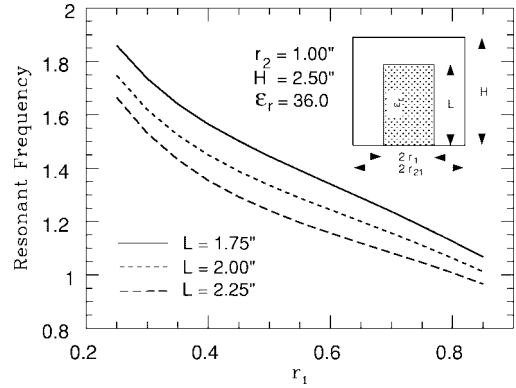


Fig. 3. Resonant frequency of a dielectric combline resonator versus the radius of the dielectric rod.

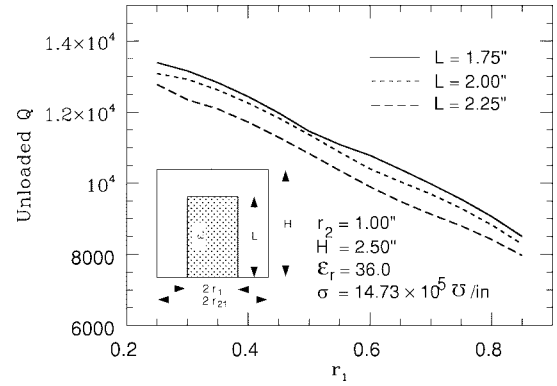


Fig. 4. Unloaded Q of a dielectric combline resonator versus the radius of the dielectric rod.

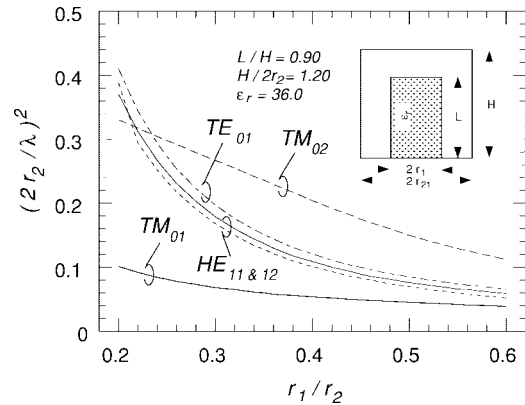


Fig. 5. Mode chart of a dielectric combline resonator with radius of the dielectric rod as variable.

the dielectric rod as variable. The fundamental mode is quite sensitive to the length of the rod, and the resonant frequency of the HE_{11} mode is relatively independent on the length. It is evident that resonators with longer rod have better spurious-free performance. The mode chart with the height of the cavity as a variable is presented in Fig. 7. The HE_{11} , HE_{12} , and TE_{01} modes are not very sensitive to the cavity height. The resonator has good mode separation when the ratio of the height of the cavity to its diameter is approximately one or greater.

All the resonators of the conventional combline filters can be fully or partially replaced by the new type of resonator. The

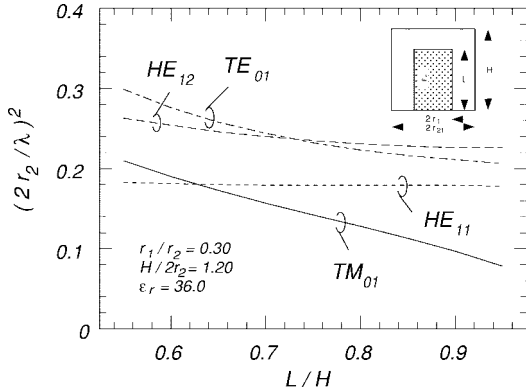


Fig. 6. Mode chart of a dielectric combline resonator with length of the dielectric rod as variable.

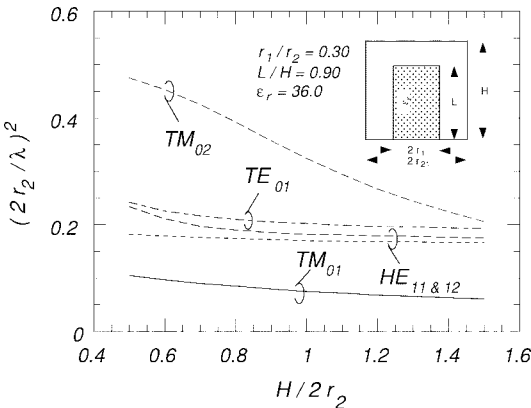


Fig. 7. Mode chart of a dielectric combline resonator with length of the dielectric rod as variable.

similarity of both types of resonators in shape, size, and field distributions provide the principal advantages of the dielectric combline resonators. The loss of a metallic combline filter will be nearly cut by half if dielectric resonators are used, while the overall filter size is kept the same. The dielectric combline resonator will have better spurious-free performance than conventional dielectric resonators. The use of some dielectric combline resonators and some metallic combline resonators in the filter will combine the superior spurious performance of the conventional combline resonators and the low-loss high-*Q* advantages of the dielectric resonators. Fig. 8 shows the typical simulated insertion loss of an eight-pole elliptic-function filter using different combination of the resonators. The results show the promising applications of the dielectric combline resonator.

IV. FILTER REALIZATION

As application of the dielectric combline resonator, an eight-pole self-equalized elliptic-function filter with center frequency of 2.595 GHz and bandwidth of 43.0 MHz using $0.75'' \times 0.75'' \times 1.40''$ size cavities was designed. The normalized input/output resistance and the coupling matrix elements of the filter are $R_{in} = R_{out} = 1.2224$, $m_{12} = m_{78} = 0.9234$, $m_{23} = m_{67} = 0.6193$, $m_{34} = m_{56} = 0.5442$, $m_{45} = 0.6957$, $m_{18} = 0.0292$, $m_{27} = -0.0518$, and $m_{36} = -0.1207$.

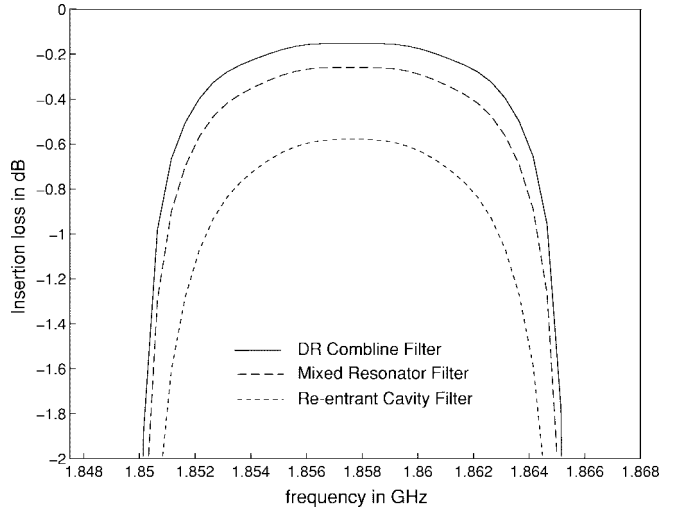


Fig. 8. Insertion loss of the eight-pole filter using different kind of resonators.

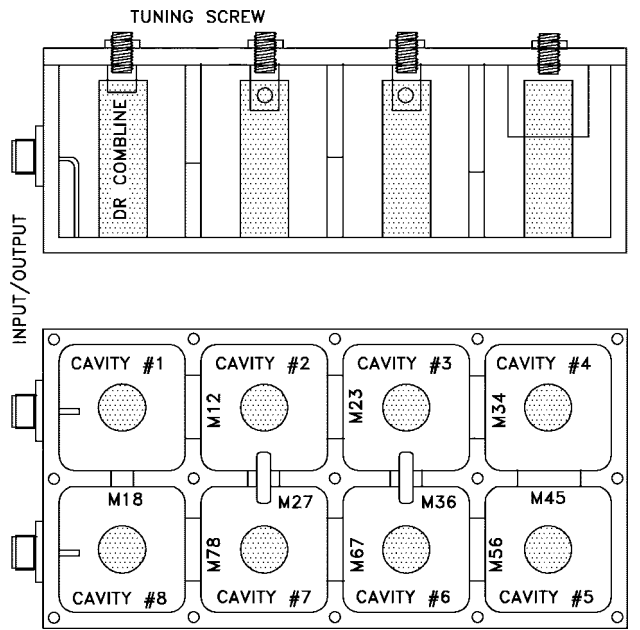


Fig. 9. Configuration of the eight-pole elliptic-function dielectric-combline-resonator filter.

The configuration of the filter is shown in Fig. 9. In the filter, the positive couplings are achieved by irises, and the negative couplings are obtained by probes. The dimensions of the resonators and irises are determined by a computer program using the modeling method described above. Tuning screws are used for fine tuning the resonant frequencies of the resonators. Fig. 10 presents the measured frequency responses of the designed filter. Fig. 11 shows the enlarged in-band insertion loss of the filter. It is seen that the filter achieves 0.75-dB insertion loss and more than 20-dB return loss. The realized *Q* of the resonator is estimated to be 4200, which is about 35% higher than the realized *Q* of 3100 of the metallic combline resonator of the same cross section [16].

Fig. 12 gives the wide-band frequency response of the filter. It is seen the closest spurious response is about 1.6 GHz

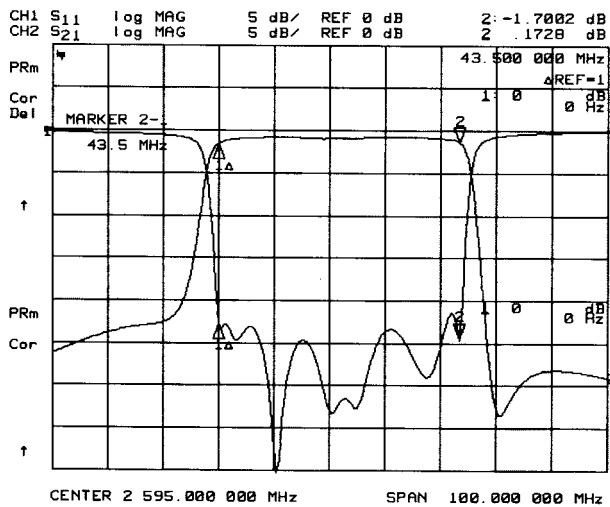


Fig. 10. Measured frequency responses of the eight-pole elliptic-function dielectric-combline-resonator filter.

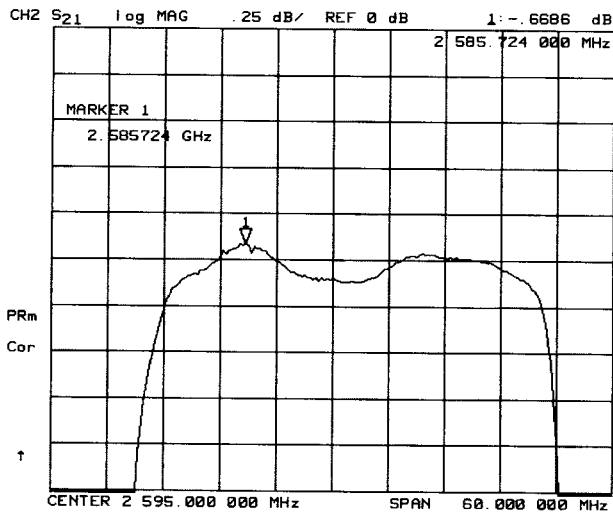


Fig. 11. Measured in-band insertion loss of the filter.

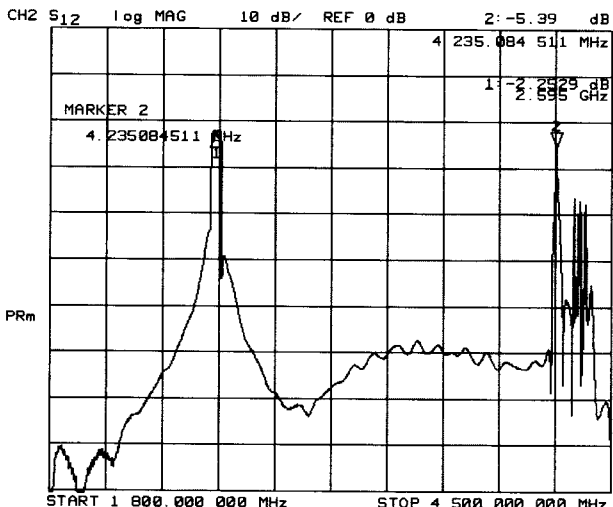


Fig. 12. Wide-band frequency responses of the filter.

higher than center frequency. The new type of filter has much better spurious performance than conventional dielectric loaded resonator ones. By combining the dielectric combline resonators with the conventional metallic combline resonators in the filter, better spurious performance can be achieved.

V. CONCLUSIONS

A new type of dielectric resonator, i.e., dielectric combline resonator, is introduced by replacing the inner conductor rod of the conventional combline resonator by a high ϵ_r dielectric rod. Properties of the new type of resonator are investigated. The resonant frequency, field distribution, unloaded Q , and the coupling coefficient of the resonator are obtained by a rigorous mode-matching method. An eight-pole self-equalized elliptic-function dielectric-combline-resonator filter was designed. Measured frequency responses verify the theory. The resonator shows the promising applications in the communication systems.

REFERENCES

- [1] G. L. Matthaei, "Comb-line band-pass filters of narrow or moderate bandwidth," *Microwave J.*, vol. 6, pp. 82-91, Aug. 1963.
- [2] R. Levy and J. D. Rhodes, "A comb-line elliptic filter," *IEEE Trans. Microwave Theory Tech.*, vol. MTT-19, pp. 26-29, Jan. 1971.
- [3] S. B. Cohn, "Microwave bandpass filters containing high- Q dielectric resonators," *IEEE Trans. Microwave Theory Tech.*, vol. MTT-16, pp. 218-227, Apr. 1968.
- [4] W. H. Harrison, "A miniature high- Q bandpass filter employing dielectric resonators," *IEEE Trans. Microwave Theory Tech.*, vol. MTT-16, pp. 210-218, Apr. 1968.
- [5] S. J. Fieduszko, "Dual-mode dielectric resonator loaded cavity filter," *IEEE Trans. Microwave Theory Tech.*, vol. MTT-30, pp. 1311-1316, Sept. 1982.
- [6] S.-W. Chen and K. A. Zaki, "Dielectric ring resonators loaded in waveguide and on substrate," *IEEE Trans. Microwave Theory Tech.*, vol. 39, pp. 2069-2076, Dec. 1991.
- [7] Y. Kobayashi and M. Minegishi, "Precise design of a bandpass filter using high- Q dielectric resonators," *IEEE Trans. Microwave Theory Tech.*, vol. MTT-35, pp. 1156-1187, Dec. 1987.
- [8] M. Sagawa, M. Makimoto, and S. Yamashita, "A design method of bandpass filter using dielectric-filled coaxial resonators," *IEEE Trans. Microwave Theory Tech.*, vol. MTT-33, pp. 152-157, Feb. 1985.
- [9] K. Hano, H. Kohriyama, and K.-I. Sawamoto, "A direct-coupled $\lambda/4$ -coaxial resonator bandpass filter for land mobile communications," *IEEE Trans. Microwave Theory Tech.*, vol. MTT-34, pp. 972-976, Sept. 1986.
- [10] X. P. Liang and K. A. Zaki, "Modeling of cylindrical dielectric resonators in rectangular waveguides and cavities," *IEEE Trans. Microwave Theory Tech.*, vol. 41, pp. 2174-2181, Dec. 1993.
- [11] H.-W. Yao, K. A. Zaki, A. E. Atia, and R. Hershtig, "Full wave modeling of conducting posts in rectangular waveguides and its applications to slot coupled combline filters," *IEEE Trans. Microwave Theory Tech.*, vol. 43, pp. 2824-2830, Dec. 1995.
- [12] C. Wang, K. A. Zaki, and A. E. Atia, "Dual mode conductor loaded cavity filters," *IEEE Trans. Microwave Theory Tech.*, vol. 45, pp. 1240-1246, Aug. 1997.
- [13] R. Levy, "Improved single and multiaperture waveguide coupling theory, including explanation of mutual interactions," *IEEE Trans. Microwave Theory Tech.*, vol. MTT-28, pp. 331-338, Apr. 1980.
- [14] H.-W. Yao, J.-F. Liang, and K. A. Zaki, "Accuracy of coupling computations and its application to DR filter design," in *IEEE MTT-S Int. Microwave Symp. Dig.*, June 1994, vol. pp. 723-726.
- [15] G. L. Matthaei, L. Young, and E. M. T. Jones, *Microwave Filters, Impedance-Matching Networks and Coupling Structure*. New York: McGraw-Hill, 1984.
- [16] H.-W. Yao, "EM simulation of resonant and transmission structures—Applications to filters and multiplexers," Ph.D. dissertation, Univ. Maryland at College Park, College Park, MD, pp. 91-108, 1995.

Chi Wang (S'95–M'97–SM'98), for photograph and biography, see this issue, p. 2411.

Kawthar A. Zaki (SM'85–F'91), for photograph and biography, see this issue, p. 2411.

Ali E. Atia (S'67–M'69–SM'78–F'87) received the B.S. degree from the Ain Shams University, Cairo, Egypt, in 1962, and the M.S. and Ph.D. degrees from the University of California at Berkeley, in 1966 and 1969, respectively, all in electrical engineering.

Prior to joining COMSAT in 1969, he held various research and teaching positions at both Ain Shams University and the University of California at Berkeley. As a Senior Scientist in the Microwave Laboratory, COMSAT Laboratories, he has made original contributions to satellite transponders and antenna technologies, most notably the development of the dual-mode microwave filters technology. He has also made significant contributions to several satellite programs. As Senior Director in the COMSAT Systems Division, he was responsible for communications systems design, integration, implementation, and testing. From 1989 to 1994, he served as the Vice President and Chief Engineer for COMSAT Technology Services. In 1994, he joined CTA Incorporated, as President of CTA International. He is currently the Senior Vice President of Communication Systems at Orbital Sciences Corporation, Germantown, MD.

Dr. Atia is a fellow of the AIAA and a member of Sigma Xi. He was a joint recipient of the 1997 Microwave Pioneer Award.

Tim G. Dolan received the B.S. degree in electrical engineering from Pennsylvania State University, University Park, in 1982.

He possesses over 15 years experience in the electronics field. For the last five years, he has been with K&L Microwave Inc., Salisbury, MD, where he is currently the Vice President of Engineering. His responsibilities include research and development and corporate administration of the engineering department. He is still involved in the design of components and systems.